A combined theoretical and experimental investigation of the kinetics and dynamics of the O(1 D) + D 2 reaction at low temperature

Dianailys Nuñez-Reyes, Kevin Hickson, Pascal Larrégaray, Laurent Bonnet, Tomás González-Lezana, Yury Suleimanov

Benchmarking Theoretical Methods through Comparison with Experiment. Kinetics and Dynamics of the $O(^1D) + D_2$ Reaction at Low Temperature

Dianailys Nuñez-Reyes,[a,b] Kevin M. Hickson,[a,b] Pascal Larrégaray,[a,b] Laurent Bonnet,[a,b] Tomás González-Lezana[c] and Yury V. Suleimanov[d,e]

[a]*Université de Bordeaux, Institut des Sciences Moléculaires, F-33400 Talence, France*

[b]*CNRS, Institut des Sciences Moléculaires, F-33400 Talence, France*

[c]*Instituto de Física Fundamental, CSIC, IFF-CSIC Serrano 123, 28006 Madrid*

[d]*Computation-based Science and Technology Research Center, Cyprus Institute, 20 Kavafi Str., Nicosia 2121, Cyprus*

[e]*Department of Chemical Engineering, Massachusetts Institute of Technology, 77 Massachusetts Ave., Cambridge, Massachusetts 02139, United States*

TOC Entry

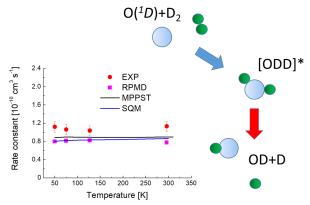

Rate constant calculations by the MPPST, SQM and RPMD methods accurately reproduce the measured values down to low temperature.

Abstract

The $O(^1D) + H_2$ reaction is a prototype for simple atom-diatom insertion type mechanisms considered to involve deep potential wells. While exact quantum mechanical methods can be applied to describe the dynamics, such calculations are challenging given the numerous bound quantum states involved. Consequently, efforts have been made to develop alternative theoretical strategies to portray accurately the reactive process. Here we report an experimental and theoretical investigation of the $O(^1D) + D_2$ reaction over the 50-296 K range. The calculations employ three conceptually different approaches – mean potential phase space theory, the statistical quantum mechanical method and ring polymer molecular dynamics. The calculated rate constants are in excellent agreement over the entire temperature range, exhibiting only weak temperature dependence. The agreement between experiment and theory is also very good, with discrepancies smaller than 26 %, thereby validating the hypothesis that long-lived complex formation dominates the reaction dynamics at low temperature.

Introduction

Atomic oxygen is an important species in the chemistry of the interstellar medium,[1] in planetary atmospheres[2] and in combustion.[3] Oxygen atoms in their ground triplet state, $O(^3P)$, participate in reactions which contribute to the Ox, NOx, HOx and ClOx budgets of the Earth's atmosphere[4] and radical-radical reactions such as $O(^3P) + OH \rightarrow O_2 + H$ are important for the transformation of atomic to molecular oxygen in interstellar clouds.[5] Although oxygen atoms in their first excited singlet state, $O(^1D)$, are characterized by a long radiative lifetime,[6] it is too short for these atoms to play a meaningful role in the chemistry of the dense interstellar medium. In planetary atmospheres, the photodissociation of oxygen bearing molecules can yield high fractional abundances of $O(^1D)$ atoms. In this respect, excited state atomic oxygen reactions have a clear impact on the overall chemistry. A well-known example is that of the reactions of $O(^1D)$ atoms with H_2O, H_2 and CH_4 reaction above the Earth's tropopause to form hydroxyl radicals that participate in the catalytic destruction of stratospheric ozone. Surprisingly, there are relatively few kinetics measurements of the $O(^1D) + H_2$ reaction and its deuterated counterparts, with most previous experiments having been performed at 300 K.[7-12] Temperature dependent rate constants have been recorded for the $O(^1D) + H_2$ reaction over the combined 50-420 K range,[13-16] but only room temperature values exist for the other isotopologues. In contrast, the dynamical aspects of the $O(^1D) + H_2$ reaction and its deuterated counterparts have been studied experimentally[17-27] and theoretically[18,20-22,28-47] on numerous occasions due to their fundamental importance as examples of atom-diatom insertion reactions involving deep potential wells. As large numbers of bound quantum states are supported in these systems, the application of exact quantum mechanical (QM) methods is computationally expensive, particularly when several potential energy surfaces (PESs) are involved. As a result, considerable effort has been devoted to finding approximate theoretical strategies which might adequately describe the dynamics of these systems.

One relatively simple approach that could be applied to such systems is Mean Potential Phase Space Theory (MPPST).[48] It relies on the assumption of complex-forming dynamics for the reaction, the states of the intermediate complex being statistically populated. Dynamical observables are then predicted from the calculation of individual capture probabilities from the reactant and product states. In MPPST, the inter-fragment interaction is averaged over the Jacobi angle. It is thus assumed to be isotropic so that capture probabilities can be described by semi-classical two-body capture models,[49] including quantization of reactant/product states and tunneling through centrifugal barriers.[50,51]

The statistical quantum method (SQM),[52] also developed under the assumption of complex-forming dynamics for the reaction, involves the calculation of individual capture probabilities by means of rigorous QM techniques on full *ab initio* PESs. The application of both MPPST and SQM to a large list of atom-diatom reactions[53] have revealed their capabilities to reproduce the main dynamical features observed both in experiments and exact QM studies, thus showing the role played by insertion mechanisms in the overall dynamics of the corresponding reactive processes.

Ring polymer molecular dynamics (RPMD) rate theory is an alternative approach that has been developed[54] and extensively benchmarked[16,55-71] over the past decade. It is based on the classical isomorphism between a quantum system and its *n* classical copies forming a necklace and coupled to its nearest neighbors via harmonic interactions. The classical isomorphism allows us to switch from a purely quantum formalism to a purely classical one and is an exact approach for calculating various static properties in which *n* – the number of beads in the necklace – is a convergence parameter. The real-time dynamics of this necklace 'ring polymer' represents an *ad hoc* idea of RPMD[54] to calculate approximately real-time correlation functions responsible for describing various dynamical processes, including chemical reactions.[56-58] Extensive studies of elementary gas-phase reactions have shown[55] that such approximations

allow QM effects of nuclear motions to be captured precisely, providing reliable and accurate estimates of thermal rate constants for different energy profiles along chemical reaction paths and over a wide range of temperatures. The key features of RPMD that lead to such success are (i) exact classical high-temperature limit, (ii) independence of the choice of transition state dividing surface, and (iii) connection to various transition state theories in the short-time limit.[55]

In this paper, we report a combined experimental and theoretical investigation of the $O(^1D) + D_2$ reaction at low temperature. There has been significant debate regarding the dynamical aspects of the $O(^1D) + H_2$ reaction and isotopic variants[53] where reaction is thought to occur predominantly over the ground state $1^1A'$ PES through the formation of an H_2O intermediate, 703 kJ mol^{-1} below the reagent level. The precise roles played by excited electronic states in different energy regimes are thought to be relevant considerations to distinguish the mechanisms governing the overall reaction dynamics. In a previous study of the $O(^1D) + H_2$ reaction,[16] thermal rate constants derived by the RPMD method over the $1^1A'$ and $1^1A''$ PESs were shown to be in reasonably good agreement with measured values down to 50 K. As the $1^1A''$ surface was shown to contribute negligibly to the overall reactivity below room temperature, these authors hypothesized that the difference between measurements and the RPMD results could be due to coupling between the $1^1A'$ and $2^1A'$ states. Indeed, precise QM wave packet (WP) calculations[44] of the $O(^1D) + H_2$ system have suggested that this nonadiabatic pathway could contribute significantly to the overall reactivity. For the $O(^1D) + D_2$ reaction, an analysis of OD product distributions from H(D)-Rydberg 'tagging' time-of-flight experiments[28] at collision energies within the range 2.0 - 3.2 kcal/mol revealed a transition between complex-forming dynamics at lower energy to an abstraction process at higher energy. Similarly, the quasi-classical trajectory (QCT) investigation of Aoiz *et al.*[72] observed an increase in the backward scattering component of the differential cross section (DCS) for increasing collision energies (86.7 - 138.8 meV); a finding which is indicative of the appearance of an abstraction

type mechanism and a larger contribution from the $1^1A''$ PES. In this sense, the experimental results presented here and the comparison with theoretical methods designed to treat complex-forming reactions, constitute a rigorous test of the overall dynamics of the $O(^1D) + D_2$ reaction at low temperature.

On the theoretical side, the MPPST, SQM and RPMD methods were employed to describe the reaction dynamics over the $1^1A'$ PES and to furnish thermal rate constants down to 50 K. RPMD calculations were also performed over the $1^1A''$ PES. In a similar manner to our earlier investigation of the $O(^1D) + H_2$ reaction,[16] these results confirm its negligible contribution to the overall reactivity at room temperature and below. To validate the theoretical approaches, rate constants were measured over the 50-296 K range using a supersonic flow reactor by following the kinetics of $O(^1D)$ loss.[73] Sections 2 and 3 describe respectively the experimental and theoretical methods used in this work. The results are discussed in section 4 and our conclusions are presented in section 5.

2 Experimental Methods

All measurements were performed using a continuous supersonic flow (Laval nozzle) reactor. The experimental setup has been described in earlier papers,[74,75] while modifications that allowed the kinetics of atom-molecule reactions to be studied are described in more recent work.[16,69,70,73,76-84] In an identical manner to previous investigations of excited state atom reactions,[16,69,70,73,76,79,82-84] only Laval nozzles employing argon were used for these experiments as a result of the fast electronic quenching of $O(^1D)$ atoms by carrier gases such as N_2.[73] These Ar based nozzles allowed uniform supersonic flows to be generated at specified temperatures of 50 K, 75 K and 127 K, with calculated densities in the range (1.26 - 2.59) × 10^{17} cm^{-3} and flow velocities between 419 and 505 ms^{-1}. The calculated and measured characteristics of the three nozzles used in this work are given in Table 1 of Grondin et al. 2016.[73] In addition to the low temperature experiments, kinetic measurements were also

performed at 296 K by removing the Laval nozzle and by reducing the flow velocity, effectively using the apparatus as a slow-flow reactor. Nevertheless, the flow velocity (73 cm s^{-1}) was still high enough to ensure that the gas in the probe region was always replenished between laser shots.

$O(^1D)$ atoms were generated in an identical manner to our other recent studies of $O(^1D)$ reactivity[16,73,83] through the pulsed laser photolysis of ozone (O_3) at 266 nm with an energy of ~23 mJ. $O(^1D)$ atoms were detected through resonant pulsed vacuum ultraviolet laser induced fluorescence (VUV LIF) at 115.215 nm via the $O(^1D)$ $3s\ ^1D - 2p\ ^1D$ transition. The procedure to generate tunable light at this wavelength by frequency tripling has already been described by Grondin et al.[73] Nevertheless, a change in the composition of the rare gas mixture used in the tripling cell (75 Torr of xenon and 155 Torr of argon) was found to yield approximately 30 % higher fluorescence signals compared to earlier work using 100 Torr of xenon and 230 Torr of argon. The present VUV LIF collection optics and solar blind photomultiplier tube (PMT) are identical to those used in the recent work of Hickson and Suleimanov.[16]

The output of the PMT was connected to a boxcar integrator for signal processing and acquisition with the acquisition electronics, lasers and oscilloscope being synchronized by a delay generator operating at 10 Hz. Each time point consisted of 30 individual laser shots, with at least 50 time intervals recorded for each $O(^1D)$ decay profile. Time points recorded with the probe laser firing at negative delays with respect to the photolysis laser allowed the pre-photolysis baseline level (consisting mostly of scattered light from the probe laser) to be evaluated.

The gases used in the experiments (O_2 (99.999%), Ar (99.999%), D_2 (99.8%) and Xe (99.998%) were not purified prior to use. All flows were controlled by calibrated digital mass flow controllers. To derive rate constants for the $O(^1D) + D_2$ reaction required a precise knowledge of the D_2 concentration in the supersonic flow. This quantity was determined from its flow ratio

(F_{D2}/F_{tot}) multiplied by the calculated total flow density. It was always several orders of magnitude larger than the estimated O(^{1}D) concentration so that pseudo-first-order conditions could be assumed for all measurements. Due to inefficient gas-phase spin conversion, the D_2 used in the present experiments was characterized by a fixed ortho/para ratio of 2:1 at all temperatures.

3 Theoretical Methods

Statistical Quantum Mechanics

The SQM method has been used before in a series of investigations focused on complex-forming reactions.[52,53,85,86] Assuming that the reaction proceeds via the formation of an intermediate species between reagents and products, the state-to-state probability can be approximated using the following expression[52]:

$$\left|S^J_{vj\Omega,v'j'\Omega'}(E)\right|^2 \approx \frac{p^J_{vj\Omega}(E)\cdot p^J_{v'j'\Omega'}(E)}{\sum_{v''j''\Omega''} p^J_{v''j''\Omega''}(E)} \qquad (1)$$

where $vj\Omega$ and $v'j'\Omega'$ refer, respectively, to the initial and final rovibrational state of D_2, indicating the quantum numbers for vibrational, rotational and third component of the angular momentum; the $p^J(E)$ quantities correspond to the probability to form the complex from the initial state at the collision energy E and for the total angular momentum J. The sum in the denominator of Eq. (1) runs for all energetically open rovibrational states at the energy E for both reagent and product channels. Using the above expression for the reaction probability, it is then possible to calculate the corresponding integral cross section, $\sigma_{vj\,v'j'}(E)$ and then the thermal rate constant:

$$k_{vj,v'j'}(T) = \sqrt{\frac{8\beta^3}{\pi\mu}}\int_0^\infty \sigma_{vj,v'j'}(E)e^{-\beta E}EdE \qquad (2)$$

where we have defined $\beta = (k_B T)^{-1}$.

Here, statistical calculations have been performed on the ground ^{1}A' PES of Dobbyn and Knowles[87,88] and the capture probability calculation of Eq. (1) has been achieved using the time-

independent propagation described in Ref. 52 in a region defined between R_c (the distance at which the D_2O complex is supposed to form) and R_{max} (an asymptotic distance) with values 1.9 Å (2.5 Å) and 27.8 Å (36.9 Å), respectively for reagents (products). SQM calculations for both j=0 and j=1 initial rotational states of D_2 have been performed and total cross sections have been calculated considering the usual 2/3 and 1/3 coefficients for the $D_2(j=0)$ and $D_2(j=1)$ populations respectively, a ratio which describes reasonably well the actual experimental conditions. The centrifugal sudden approximation[52] provides good enough results in comparison with the coupled-channel version of the SQM approach and it suffices for the presently investigated collision energy range (10-5 eV-0.4 eV).

Mean Potential Phase Space Theory

MPPST is based on a semi-classical statistical approach for atom-diatom reaction.[89,90] It uses the same statistical assumptions for the intermediate complex states as the SQM method. However, capture probabilities from the asymptotic semi-classically quantized (v, j, l) states are computed in an approximate manner. For barrierless processes, such as the one studied here, the reactant/product channel anisotropies are expected to be moderate. Consequently, the inter-fragment potential might be assumed to be isotropic: anisotropy is implicitly considered by averaging the *ab initio* PES over the reactant γ Jacobi angle in attractive regions for the ^{1}A' $O(^1D) + D_2$ and OD + D channels.[87,88] Capture probabilities are then computed via a two-body capture model[49] accounting for possible tunneling through the radial effective potential through the Wentzel-Kramers-Brillouin (WKB) model[50,51] and used in eqs. 1 and 2.[48] A simplified classical mechanical treatment of the orbital angular momentum leads to results in quantitative agreement because of subtle compensation between tunneling and quantum reflection.[51] Besides, as the process is highly exothermic (1.89 eV), the reaction cross-section equals the intermediate complex cross-section so that capture from the reactant is only needed if no information on the dynamical observables of the products is required (as is the case for the rate

constant calculations). It should be noted that, because of the isotropic assumption for the inter-fragment potential, the capture cross-section does not depend on the D_2 initial rotational state.

Ring Polymer Molecular Dynamics

In the present study, we used the RPMDrate code developed by one of us (YVS).[91] The RPMDrate computational procedure is well documented in previous studies[56-58] and in a recent review.[55] Briefly, the Bennett-Chandler factorization[92,93] is used to avoid high computational expense of the direct trajectories approach which can be prohibitive at low temperatures and/or high energy barriers. The calculation is split into two steps – the construction of the ring polymer potential of mean force W(ξ) (or free energy) profile along the reaction coordinate ξ defined using the formalism of two dividing surfaces (1)[55,56,58,91] and the ring polymer transmission coefficient κ (or recrossing factor) calculation (2). These steps are usually performed sequentially to detect the maximum value of the free energy during the first step and to initiate the recrossing factor calculations from this point during the second step. This allows recrossings to be minimized (thereby avoiding the issue of converging small values of κ) and the propagation time required to achieve the plateau value of κ to be optimized. For thermally activated energy profiles, the free energy barrier is located near the classical saddle point configuration while for reactions of insertion type it is usually located prior to the complex (deep well) and is due to the entropic factor.[55]

Theoretical RPMD rate constants were obtained using the two lowest PESs $1^1A'$ and $1^1A''$ which possess barrierless and thermally activated energy profiles, respectively. In the present study, we employed the Dobbyn-Knowles surfaces.[87,88] The input parameters are summarized in Table S1 along with the intermediate RPMD results such as the potential of mean force (Figure S1) and the transmission coefficient (Figure S2) which are similar to the results previously obtained for the $O(^1D) + H_2$ reaction.[16] The final results of the present RPMD calculations are summarized in Table S2.

4 Results and Discussion

The possible complex-forming character of the $O(^1D) + H_2$ reaction has already been investigated by statistical methods.[45,46,52,53] The calculated rovibrational cross sections and DCSs compared favourably with both exact QM and experimental results at E_c = 56 meV, suggesting that the dynamical features observed at this collision energy resulted predominantly from an insertion mechanism. A statistical description of the dynamics below 150 meV was also performed in a previous study of the $O(^1D) + H_2$ reaction, including a comparison of rate constants derived by the SQM and MPPST methods with exact QM and experimental results.[45] An equivalent study can be performed for the $O(^1D) + D_2$ system, comparing statistical predictions with previous work. QM reaction probabilities obtained by Pradhan *et al*.[94] for a zero total angular momentum $J = 0$ using the same $1^1A'$ PES[87,88] are reasonably well described by the MPPST and SQM approaches as can be seen in Figure 1.

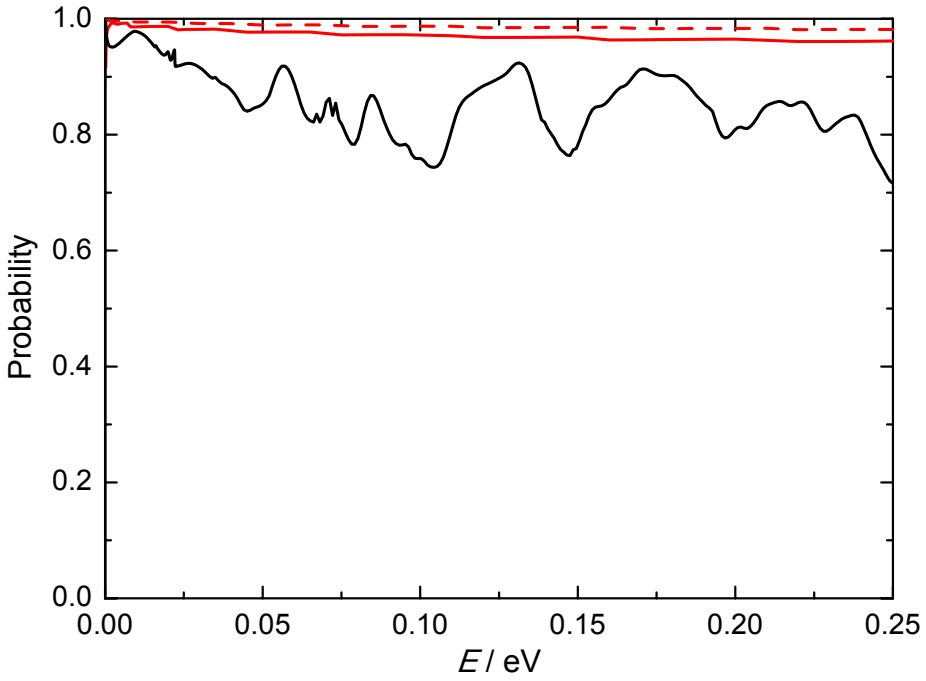

Figure 1 Total reaction probability for $O(^1D) + D_2$ as a function of the collision energy for zero total angular momentum ($J = 0$). (Solid black line) Pradhan et al.[94] $O(^1D) + D_2$ ($v = 0$, $j = 0$); (Red dashed line) MPPST method, this work; (Red solid line) SQM method, this work.

The statistical probabilities of 0.96-0.98 are only slightly above the QM results. Figure 2 shows experimental DCSs for the $O(^1D) + D_2$ reaction at E_c = 0.104 eV (top panel) and 0.228 eV (bottom panel) taken from Ahmed et al.[95] and Alagia et al.[18], respectively.

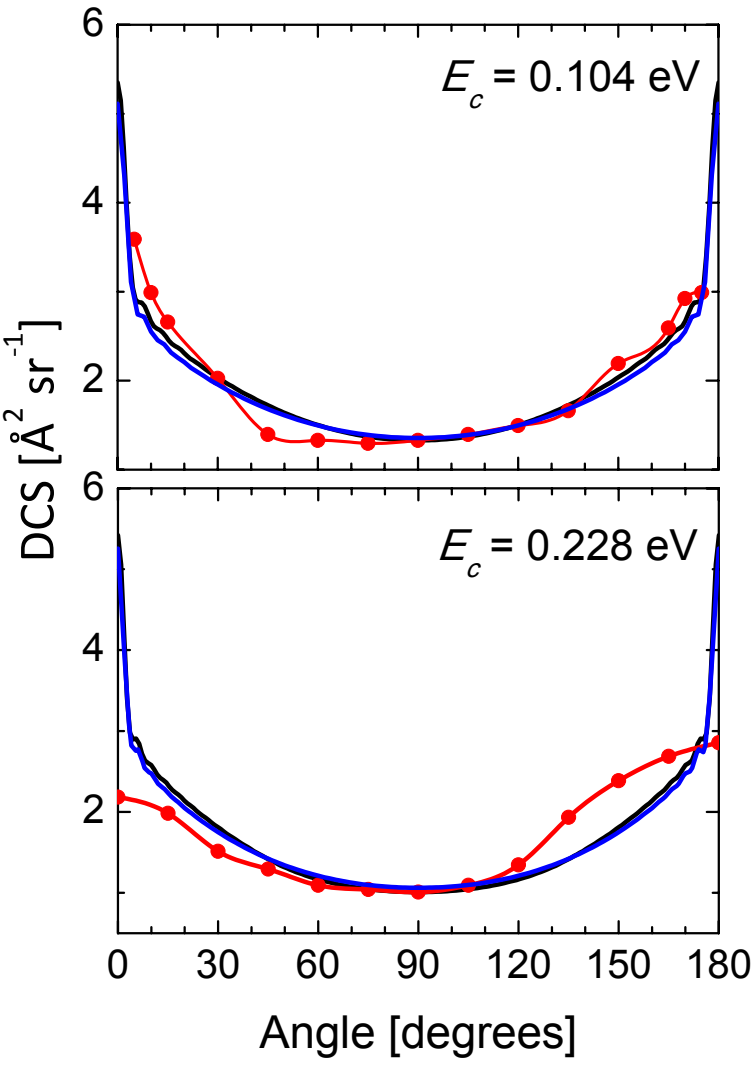

Figure 2 Differential cross sections for the $O(^1D) + D_2$ reaction at 0.104 eV (top) and 0.228 eV (bottom) collision energy. Black lines are present SQM results, blue lines are present MPPST results and red lines are experimental results from Ahmed et al.[95] (top) and Alagia et al.[18] (bottom), conveniently scaled here to match the theoretical values at the sideways scattering direction, 90 degrees.

The corresponding SQM and MPPST angular distributions, also shown, agree well at lower collision energy (see top panel). DCSs calculated with a QCT approach by Rio and Brandao[32] at the same energies (not shown here) were obtained using a different PES[96] and are slightly larger than present statistical distributions. Although measurements were not performed at the forward (90º) and backward (180º) scattering directions, the accord with the theoretical distributions over the rest of the angular range is remarkable. Noticeable deviations are observed however, at higher energy (0.228 eV - bottom panel of Figure 2), a possible indication of the onset of abstraction that cannot be properly described using the statistical approaches. Indeed, QCT calculations on both ^{1}A' and ^{1}A" PESs could reproduce these experimental DCSs, showing that excited electronic states clearly contribute to the dynamics at higher energy.[47,97] Nevertheless, a similar description[26] was not possible for even larger energies, 25.9 kJ mol^{-1} (0.268 eV), with the authors concluding that further theoretical and experimental work was required.

On the experimental side, the O(^{1}D) VUV LIF signal was recorded as a function of time for a range of excess D_2 concentrations and in the absence of D_2. Two such decay profiles are displayed in Figure 3A for experiments conducted with $[D_2] = 1.1 \times 10^{15}$ cm^{-3} and without D_2.

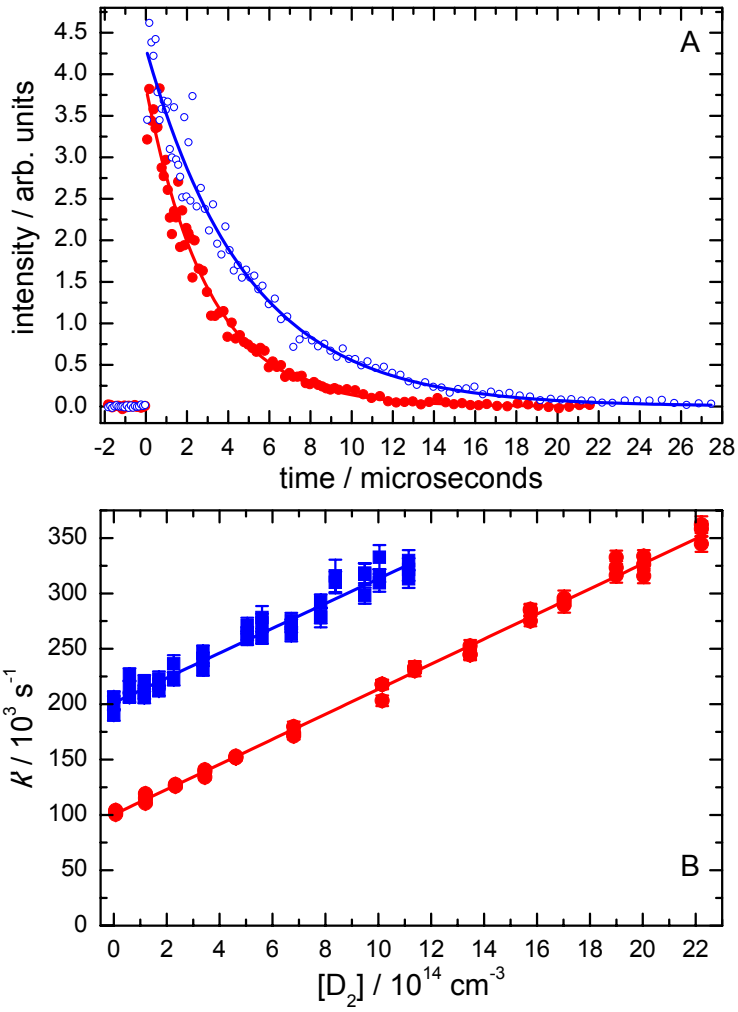

Figure 3 (A) O(^{1}D) VUV LIF signal as a function of time at 50 K. (Red solid circles) [D_2] = 1.1 × 10^{15} cm^{-3}; (blue open circles) without D_2. The fits are represented by solid blue and red lines using an expression of the form $I_{O(^1D)} = I_{O(^1D)_0} exp(-k't)$. (B) Measured pseudo-first-order rate constants as a function of [D_2]. (Red solid circles) 296 K experiments; (blue solid squares) 50 K experiments. Error bars were derived from single-exponential fits to the individual O(^{1}D) decays and are cited at the level of a single standard deviation. Second-order rate constants were derived from weighted fits to the data (solid red and blue lines).

In the absence of D_2, the O(^{1}D) VIV LIF signal decays exponentially to zero as a function of time through non-reactive quenching collisions with the carrier gas Ar. When D_2 is added to the system, O(^{1}D) atoms are removed from the flow by reaction with D_2 in addition to

quenching by Ar. A function of the type $I_{O(^1D)} = I_{O(^1D)_0} exp(-k't)$, where t is time and $I_{O(^1D)}$ and $I_{O(^1D)_0}$ are the time dependent and initial O(^{1}D) VUV LIF intensities (which are proportional to the O(^{1}D) concentration) was used to perform a non-linear least-squares fit to the data. This allowed the pseudo-first-order rate constants for O(^{1}D) removal, k', to be extracted from the time constants of the decays. In the present experiments, k' is essentially equal to the sum of two contributions (see Grondin et al.[73] for a more detailed analysis), $k' = k_{O(^1D) + Ar}[Ar] + k_{O(^1D) + D_2}[D_2]$ where $k_{O(^1D) + Ar}$ and $k_{O(^1D) + D_2}$ are the second-order rate constants for O(^{1}D) removal by Ar and D_2 respectively. Plotting k' as a function of [D_2] thus allows us to determine $k_{O(^1D) + D_2}$ from a weighted linear least-squares fit to the data. Representative second-order plots obtained at 296 K and at 50 K are shown in Figure 3B and at 127 K and 75 K in Figure S3. In these examples, the large y-intercept value represents the quenching contribution of the carrier gas Ar, $k_{O(^1D) + Ar}[Ar]$. The measured second-order rate constants are listed in Table S3 and displayed as a function of temperature in Figure 4 alongside the present theoretical results and earlier work.

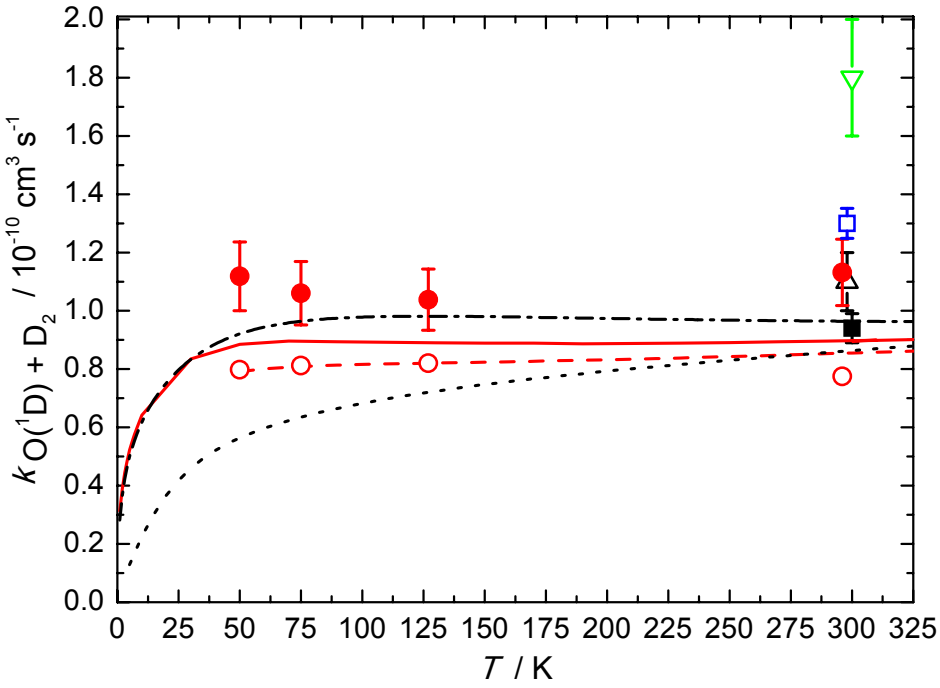

Figure 4 Rate constants for the $O(^1D) + D_2$ reaction as a function of temperature. Experimental values: (Green inverted open triangle) Heidner and Husain[7]; (blue open square) Davidson et al.[98]; (black solid square) Matsumi et al.[24]; (black open triangle) Talukdar and Ravishankara[12]; (red solid circle) this work. Theoretical values: (dashed dotted black line) QM results of Pradhan et al.[94]; (dotted black line) QM results of Sun et al.[99]; (solid red line) this work, MPPST method; (dashed red line) this work, SQM method; (red open circles) this work, RPMD method.

There are several earlier room temperature measurements of the rate constant for the $O(^1D) + D_2$ reaction.[7,12,24,98] The experimental rate constant of $(1.13 \pm 0.11) \times 10^{-10}$ cm^3 s^{-1} determined at 296 K in the present work is in excellent agreement with all but one of these previous investigations.[7] Considering the error bars, the present rate constants are found to be independent of temperature over the 50-296 K range; in good qualitative agreement with our recent investigation of the $O(^1D) + H_2$ reaction over the same range.[16] Figure 4 also contains the results of previous theoretical investigations of the title reaction.[94,99] The agreement between the present experimental results and both the QM rate constants of Pradhan *et al.*[94] and all the approximate theoretical approaches employed here is very good, strongly supporting the

involvement of a long-lived intermediate complex in the dynamics of the $O(^1D) + D_2$ reaction in this low temperature regime. Interestingly, the rate constants derived by Pradhan *et al.*[94] are approximately 10 % lower than the experimental ones, with an identical difference having also been observed in the case of the $O(^1D) + H_2$ reaction.[16,100]

As rate constants have already been measured for the $O(^1D) + H_2$ reaction over the same temperature range and calculated using all three theoretical methodologies employed here,[16,45] we can also evaluate the temperature dependent kinetic isotope effect (KIE) (defined as the ratio of the rate constants, $k_{O(^1D)+D_2}/k_{O(^1D)+H_2}$, at a given temperature). The derived KIE values are compared with previous experimental and theoretical work for these systems in Figure 5.

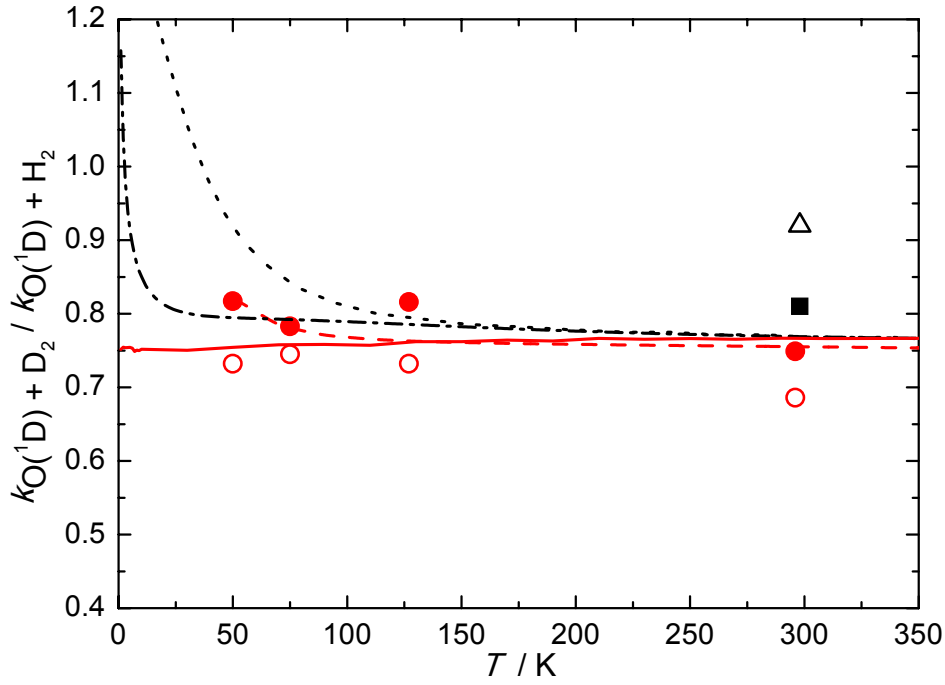

Figure 5 Kinetic isotope effect (KIE), $k_{O(^1D)+D_2}/k_{O(^1D)+H_2}$, as a function of temperature. Experimental values: (black solid square) Hsu et al.[23]; (black open triangle) Talukdar and Ravishankara[12]; (red solid circle) this work. Theoretical values: (dashed dotted black line) QM results of Pradhan et al.[94,100]; (dotted black line) QM WP results of Sun et al.[99] / QM WP results

of Lin and Guo[44]; (solid red line) this work, MPPST method; (dashed red line) this work, SQM method; (red open circles) this work, RPMD method.

The present experimental and theoretical KIE values agree very well with the experimental value of 0.81 determined by Hsu et al.[23] at higher equivalent temperatures. They are also in excellent agreement above 100 K with the previous theoretical values derived from the ratio of the rate constants obtained by the Sun et al.[99] and Lin and Guo[44] QM WP investigations of the $O(^1D) + D_2$ and H_2 reactions respectively over three PESs. While the experimental KIE remains constant down to 50 K, the QM WP KIE increases dramatically below 100 K. This discrepancy could be a sign of convergence issues in either or both QM WP studies at low collision energies. In contrast, the KIE derived by Pradhan et al.[94,100] using a time independent QM method and a *J*-shifting approximation is in excellent agreement with the present experimental and theoretical ones over the entire temperature range.

The comparisons shown in Figures 4 and 5 between the rate constants (KIE values) derived by exact QM methods and the equivalent values derived by the three theoretical approaches applied here validate the use of these statistical-based and approximate QM methods for an accurate description of the dynamics of complex-forming insertion type reactions in the low temperature regime. While such agreement is extremely encouraging, the present and previous calculations all slightly underestimate the measured rate constants for both the $O(^1D) + D_2$ and $O(^1D) + H_2$ reactions at low temperature. These discrepancies could have several possible origins including deficiencies in the PESs used, or they might be due to convergence issues or approximations used during the calculations. Alternatively, such differences could indicate the presence of nonadiabatic couplings in these systems that are not considered by the present calculations. Future work should focus on the inclusion of a correct treatment of nonadiabatic interactions to improve further the agreement between experiment and theory.

5 Conclusions

This work presents an experimental and theoretical investigation of the dynamics and kinetics of the gas-phase $O(^1D) + D_2$ reaction. On the experimental side, a supersonic flow reactor was used to attain temperatures as low as 50 K. $O(^1D)$ atoms were produced and detected directly in the cold flow by pulsed laser photolysis and pulsed laser induced fluorescence methods respectively. On the theoretical side, three conceptually different methodologies were used to examine the dynamics of the title reaction - Statistical Quantum Mechanics (SQM), Mean Potential Phase Space Theory (MPPST) and Ring Polymer Molecular Dynamics (RPMD). The results of both the SQM and MPPST calculations confirm that the reaction can be treated statistically and that the dominant mechanism at low temperature involves complex formation through $O(^1D)$ insertion into the D-D bond. Thermal rate constants derived by these two methods are in good agreement with the measured values. Rate constants calculated by RPMD, a more recently proposed method that has no prior assumptions regarding the reaction mechanism, were also in good agreement demonstrating the suitability of this technique for the investigation of insertion reactions down to low temperature. It is argued that the slight discrepancies between theoretical and experimental results could arise either from deficiencies in the present calculations such as approximations or due to inaccuracies in the underlying potential energy surface, or from nonadiabatic effects that are not considered here.

Acknowledgments

The authors want to thank Prof. Balakrishnan for sharing his QM results. KMH acknowledges support from the French program “Physique et Chimie du Milieu Interstellaire” (PCMI) funded by the Centre National de la Recherche Scientifique (CNRS) and Centre National d’Etudes Spatiales (CNES). TGL acknowledges support from MICINN with Grant FIS2014-51993-P. Y.V.S. thanks the European Regional Development Fund and the Republic of Cyprus for support through the Research Promotion Foundation (Project Cy-Tera NEA

ΥΠΟΔΟΜΗ/ΣΤΡΑΤΗ/0308/31). Y.V.S. also acknowledges the support of the COST CMTS-Action CM1401 (Our Astro-Chemical History).

Electronic supplementary information (ESI) available.

Intermediate RPMD data such as the profiles of potential of mean force (Figure S1) and transmission coefficients (Figure S2).
Experimental second-order plots recorded at 127 K and 75 K (Figure S3).
The input parameters for the RPMDrate calculations for both potential energy surfaces (^{1}A' and ^{1}A") (Table S1).
Final thermal RPMD rate constants and ring polymer recrossing factors plateau values (Table S2).
The measured second-order rate constants (Table S3).

References

1. M. Agundez and V.Wakelam, Chemistry of Dark Clouds: Databases, Networks, and Models. *Chem. Rev.* 2013, **113**, 8710-8737.

2. J. W. Stock, C. S. Boxe, R. Lehmann, J. L. Grenfell, A. B. C. Patzer, H. Rauer and Y. L. Yung, Chemical Pathway Analysis of the Martian Atmosphere: CO_2-Formation Pathways. *Icarus* 2012, **219**, 13-24.

3. D. L. Baulch, Evaluated Kinetic Data for Combustion Modeling: Supplement II. *J. Phys. Chem. Ref. Data* 2005, **34**, 757-1397.

4. S. P. Sander, J. Abbatt, J. R. Barker, J. B. Burkholder, R. R. Friedl, D. M. Golden, R. E. Huie, C. E. Kolb, M. J. Kurylo, G. K. Moortgat, V. L. Orkin and P. H. Wine, Chemical Kinetics and Photochemical Data for Use in Atmospheric Studies, Evaluation No. 17. *JPL Publication 10-6, Jet Propulsion Laboratory, Pasadena, 2011* http://jpldataeval.jpl.nasa.gov/. **2011**.

5. U. Hincelin, V. Wakelam, F. Hersant, S. Guilloteau, J. C. Loison, P. Honvault and J. Troe, Oxygen Depletion in Dense Molecular Clouds: A Clue to a Low O_2 abundance? *Astron. Astrophys.* 2011, **530**, A61.

6. J. A. Kernahan and P. H. L. Pang, Experimental Determination of Absolute A Coefficients for 'Forbidden' Atomic Oxygen Lines. *Can. J. Phys.* 1975, **53**, 455-458.

7. R. F. Heidner and D. Husain, Electronically Excited Oxygen Atoms, $O(2^1D_2)$. A Time-Resolved Study of the Collisional Quenching by the Gases H_2, D_2, CH_4, NO, NO_2, N_2O, and C_3O_2 Using Atomic Absorption Spectroscopy in the Vacuum Ultraviolet. *Int. J. Chem. Kinet.* 1973, **5**, 819-831.

8. S. T. Amimoto, A. P. Force, R. G. Gulotty and J. R. Wiesenfeld, Collisional Deactivation of $O(2^1D_2)$ by the Atmospheric Gases. *J. Chem. Phys.* 1979, **71**, 3640-3647.

9. P. H. Wine and A. R. Ravishankara, Kinetics of $O(^1D)$ Interactions with the Atmospheric Gases N_2, N_2O, H_2O, H_2, CO_2, and O_3. *Chem. Phys. Lett.* 1981, **77**, 103-109.

10. S. Koppe, T. Laurent, P. D. Naik, H. R. Volpp, J. Wolfrum, T. Arusiparpar, I. Bar and S. Rosenwaks, Absolute Rate Constants and Reactive Cross-Sections for the Reactions of $O(^1D)$ with Molecular-Hydrogen and Deuterium. *Chem. Phys. Lett.* 1993, **214**, 546-552.

11. Y. Matsumi, K. Tonokura, Y. Inagaki and M. Kawasaki, Isotopic Branching Ratios and Translational Energy-Release of H-Atoms and D-Atoms in Reaction of $O(^1D)$ Atoms with Alkanes and Alkyl Chlorides. *J. Phys. Chem.* 1993, **97**, 6816-6821.

12. R. K. Talukdar and A. R. Ravishankara, Rate Coefficients for $O(^1D)+H_2$, D_2, HD Reactions and H Atom Yield in $O(^1D)$+HD Reaction. *Chem. Phys. Lett.* 1996, **253**, 177-183.

13. J. A. Davidson, H. I. Schiff, G. E. Streit, J. R. McAfee, A. L. Schmeltekopf and C. J. Howard, Temperature Dependence of $O(^1D)$ Rate Constants for Reactions with N_2O, H_2, CH_4, HCl, and NH_3. *J. Chem. Phys.* 1977, **67**, 5021-5025.

14. M. A. Blitz, T. J. Dillon, D. E. Heard, M. J. Pilling and I. D. Trought, Laser Induced Fluorescence Studies of the Reactions of $O(^1D_2)$ with N_2, O_2, N_2O, CH_4, H_2, CO_2, Ar, Kr and N-C_4H_{10}. *Phys. Chem. Chem. Phys.* 2004, **6**, 2162-2171.

15. S. Vranckx, J. Peeters and S. Carl, Kinetics of $O(^1D) + H_2O$ and $O(^1D) + H_2$: Absolute Rate Coefficients and $O(^3P)$ Yields between 227 and 453 K. *Phys. Chem. Chem. Phys.* 2010, **12**, 9213-9221.

16. K. M. Hickson and Y. V. Suleimanov, Low-Temperature Experimental and Theoretical Rate Constants for the $O(^1D) + H_2$ Reaction. *J. Phys. Chem. A* 2017, **121**, 1916-1923.

17. R. J. Buss, P. Casavecchia, T. Hirooka, S. J. Sibener and Y. T. Lee, Reactive Scattering of $O(^1D)+H_2$. *Chem. Phys. Lett.* 1981, **82**, 386-391.

18. M. Alagia, N. Balucani, L. Cartechini, P. Casavecchia, E. H. van Kleef, G. G. Volpi, P. J. Kuntz and J. J. Sloan, Crossed Molecular Beams and Quasiclassical Trajectory Studies of the Reaction $O(^1D)+H_2(D_2)$. *J. Chem. Phys.* 1998, **108**, 6698-6708.

19. X. Liu, C. C. Wang, S. A. Harich and X. Yang, Effect of a Single Quantum Rotational Excitation on State-to-State Dynamics of the $O(^1D)+H_2 \rightarrow OH+H$ Reaction. *Phys. Rev. Lett.* 2002, **89**, 133201.

20. F. J. Aoiz, L. Bañares, J. F. Castillo, V. J. Herrero, B. Martinez-Haya, P. Honvault, J. M. Launay, X. Liu, J. J. Lin, S. A. Harich, C. C. Wang and X. Yang, The $O(^1D)+H_2$ Reaction at 56 meV Collision Energy: A Comparison between Quantum Mechanical, Quasiclassical Trajectory, and Crossed Beam Results. *J. Chem. Phys.* 2002, **116**, 10692-10703.

21. S. K. Gray, G. G. Balint-Kurti, G. C. Schatz, J. J. Lin, X. Liu, S. Harich and X. Yang, Probing the Effect of the H_2 Rotational State in $O(^1D)+H_2 \rightarrow OH + H$: Theoretical Dynamics Including Nonadiabatic Effects and a Crossed Molecular Beam Study. *J. Chem. Phys.* 2000, **113**, 7330-7344.

22. X. H. Liu, J. J. Lin, S. Harich, G. C. Schatz and X. M. Yang, A Quantum State-Resolved Insertion Reaction: $O(^1D) + H_2 (J = 0) \rightarrow OH (^2\Pi, v, N) + H(^2S)$. *Science* 2000, **289**, 1536-1538.

23. Y. T. Hsu, J. H. Wang and K. P. Liu, Reaction Dynamics of $O(^1D)+H_2$, D_2, and HD: Direct Evidence for the Elusive Abstraction Pathway and the Estimation of its Branching. *J. Chem. Phys.* 1997, **107**, 2351-2356.

24. Y. Matsumi, K. Tonokura, M. Kawasaki and H. L. Kim, Dynamics of the Reaction $O(^1D)$ + HD, H_2, and D_2 - Isotopic Branching Ratios and Translational Energy-Release. *J. Phys. Chem.* 1992, **96**, 10622-10626.

25. P. Hermine, Y. T. Hsu and K. Liu, A Crossed-Beam Study of the Reaction $O(^1D)+D_2$: Collisional Energy Dependence of Differential Cross-Section. *Phys. Chem. Chem. Phys.* 2000, **2**, 581-587.

26. N. Balucani, P. Casavecchia, F. J. Aoiz, L. Bañares, J. F. Castillo and V. J. Herrero, Dynamics of the $O(^1D)$ + D_2 Reaction: A Comparison between Crossed Molecular Beam Experiments and Quasiclassical Trajectory Calculations on the Lowest Three Potential Energy Surfaces. *Mol. Phys.* 2005, **103**, 1703-1714.

27. S. Kauczok, C. Maul, A. I. Chichinin and K. H. Gericke, Measurement of the Differential Cross Section of the Photoinitiated Reactive Collision of $O(^1D)+D_2$ Using Only One Molecular Beam: A Study by Three Dimensional Velocity Mapping. *J. Chem. Phys.* 2010, **132**, 244308.

28. X. Liu, J. J. Lin, S. A. Harich and X. Yang, State-to-state Dynamics for $O(^1D)+D_2 \rightarrow$ OD+D: Evidence for a Collinear Abstraction Mechanism *Phys. Rev. Lett.* 2001, **86**, 408-411.

29. Y. F. Liu, Y. L. Gao, D. H. Shi and J. F. Sun, Theoretical Study of the Stereodynamics of the Reactions $O(^1D)$ + H_2, D_2 and HD. *Chem. Phys.* 2009, **364**, 46-50.

30. D. Kuang, T. Y. Chen, W. P. Zhang, N. J. Zhao and D. J. Wang, Effects of Reagent Rotation on Stereodynamics Information of the Reaction $O(^1D)+H_2$ (v=0, j=0-5) → OH + H: A Theoretical Study. *Bull. Korean Chem. Soc.* 2010, **31**, 2841-2848.

31. S. Y. Lin and H. Guo, Energy Dependence of Differential and Integral Cross Sections for $O(^1D)+H_2$ (v=0,j=0) → OH (v',j')+H Reaction. *J. Chem. Phys.* 2008, **129**, 124311.

32. C. M. A. Rio and J. Brandão, Dynamical Studies and Product Analysis of $O(^1D)$ + H_2/D_2 Reactions. *Mol. Phys.* 2007, **105**, 359-373.

33. M. H. Alexander, E. J. Rackham and D. E. Manolopoulos, Product Multiplet Branching in the $O(^1D)+H_2 \rightarrow OH(^2\Pi)+H$ Reaction. *J. Chem. Phys.* 2004, **121**, 5221-5235.

34. J. Hernando, R. Sayos and M. González, A QCT Study of the Microscopic Mechanisms Proceeding via the Ground PES of the $O(^1D) + H_2 (X^1 \sum^+_g) \rightarrow OH(X^2 \Pi)+H(^2S)$ Reaction. *Chem. Phys. Lett.* 2003, **380**, 123-134.

35. T. Takayanagi, Nonadiabatic Quantum Reactive Scattering Calculations for the $O(^1D)+H_2$, D_2, and HD Reactions on the Lowest Three Potential Energy Surfaces. *J. Chem. Phys.* 2002, **116**, 2439-2446.

36. T. E. Carroll and E. M. Goldfield, Coriolis-Coupled Quantum Dynamics for $O(^1D)+H_2 \rightarrow$ OH+H. *J. Phys. Chem. A* 2001, **105**, 2251-2256.

37. P. Honvault and J. M. Launay, A Quantum-Mechanical Study of the Dynamics of the $O(^1D)+H_2 \rightarrow OH+H$ Insertion Reaction. *J. Chem. Phys.* 2001, **114**, 1057-1059.

38. M. Hankel, G. G. Balint-Kurti and S. K. Gray, Quantum Mechanical Calculation of Product State Distributions for the $O(^1D)+H_2 \rightarrow OH+H$ Reaction on the Ground Electronic State Surface. *J. Chem. Phys.* 2000, **113**, 9658-9667.

39. A. J. Alexander, F. J. Aoiz, L. Bañares, M. Brouard and J. P. Simons, Product Rotational Angular Momentum Polarization in the Reaction $O(^1D_2) + H_2 \rightarrow OH + H$. *Phys. Chem. Chem. Phys.* 2000, **2**, 571-580.

40. S. K. Gray, E. M. Goldfield, G. C. Schatz and G. G. Balint-Kurti, Helicity Decoupled Quantum Dynamics and Capture Model Cross Sections and Rate Constants for $O(^1D)+H_2 \rightarrow OH+H$. *Phys. Chem. Chem. Phys.* 1999, **1**, 1141-1148.

41. S. K. Gray, C. Petrongolo, K. Drukker and G. C. Schatz, Quantum Wave Packet Study of Nonadiabatic Effects in $O(^1D)+H_2 \rightarrow OH+H$. *J. Phys. Chem. A* 1999, **103**, 9448-9459.

42. K. Drukker and G. C. Schatz, Quantum Scattering Study of Electronic Coriolis and Nonadiabatic Coupling Effects in $O(^1D)+H_2 \rightarrow OH+H$. *J. Chem. Phys.* 1999, **111**, 2451-2463.

43. Y. Li, Y. V. Suleimanov and H. Guo, Ring-Polymer Molecular Dynamics Rate Coefficient Calculations for Insertion Reactions: $X + H_2 \rightarrow HX + H$ (X = N, O). *J. Phys. Chem. Lett.* 2014, **5**, 700-705.

44. S. Y. Lin and H. Guo, Adiabatic and Nonadiabatic State-to-State Quantum Dynamics for $O(^1D) + H_2(X^1 \sum_g^+, v_i = j_i = 0) \rightarrow OH(X\ 2\Pi, v_f, j_f) + H(^2S)$ Reaction. *J. Phys. Chem. A* 2009, **113**, 4285-4293.

45. A. Rivero-Santamaria, M. L. González-Martínez, T. González-Lezana, J. Rubayo-Soneira, L. Bonnet and P. Larrégaray, The $O(^1D) + H_2 (X\ ^1\sum^+, v, j) \rightarrow OH(X\ ^2\Pi, v', j') + H(^2S)$ Reaction at Low Collision Energy: When a Simple Statistical Description of the Dynamics Works. *Phys. Chem. Chem. Phys.* 2011, **13**, 8136-8139.

46. E. J. Rackham, F. Huarte-Larrañaga and D. E. Manolopoulos, Coupled-Channel Statistical Theory of the $N(^2D)+H_2$ and $O(^1D)+H_2$ Insertion Reactions. *Chem. Phys. Lett.* 2001, **343**, 356-364.

47. F. J. Aoiz, L. Bañares, J. F. Castillo, M. Brouard, W. Denzer, C. Vallance, P. Honvault, J. M. Launay, A. J. Dobbyn and P. J. Knowles, Insertion and Abstraction Pathways in the Reaction $O(^1D_2) + H_2 \rightarrow OH+H$. *Phys. Rev. Lett.* 2001, **86**, 1729-1732.

48. P. Larrégaray and L. Bonnet, Rationalizing the $S(^1D)+H_2 \rightarrow SH(X\ ^2\Pi) + H$ Reaction Dynamics through a Semi-classical Capture Model. *Comp. Theo. Chem.* 2012, **990**, 18-22.

49. P. Langevin, Une Formule Fondamentale de Théorie Cinétique. *Ann. Chim. Phys.* 1905, **5**, 245-288.

50. M. S. Child, *Semiclassical Mechanics with Molecular Applications* Clarendon Press: Oxford, 1991.

51. R. Meana-Paneda, D. G. Truhlar and A. Fernandez-Ramos, Least-Action Tunneling Transmission Coefficient for Polyatomic Reactions. *J. Chem. Theo. Comp*. 2010, **6**, 6-17.

52. E. J. Rackham, T. González-Lezana and D. E. Manolopoulos, A Rigorous Test of the Statistical Model for Atom-Diatom Insertion Reactions. *J. Chem. Phys.* 2003, **119***,* 12895-12907.

53. T. González-Lezana, Statistical Quantum Studies on Insertion Reactions, *Int. Rev. Phys. Chem.* 2007, **26**, 29-91.

54. I. R. Craig and D. E. Manolopoulos, Quantum Statistics and Classical Mechanics: Real Time Correlation Functions from Ring Polymer Molecular Dynamics. *J. Chem. Phys.* 2004, **121**, 3368-3373.

55. Y. V. Suleimanov, F. J. Aoiz and H. Guo, Chemical Reaction Rate Coefficients from Ring Polymer Molecular Dynamics: Theory and Practical Applications. *J. Phys. Chem. A* 2016, **120**, 8488-8502.

56. R. Collepardo-Guevara, Y. V. Suleimanov and D. E. Manolopoulos, Bimolecular Reaction Rates from Ring Polymer Molecular Dynamics. *J. Chem. Phys.* 2009, **130**, 174713.

57. R. Collepardo-Guevara, Y. V. Suleimanov and D. E.Manolopoulos, "Erratum: Bimolecular Reaction Rates from Ring Polymer Molecular Dynamics" [*J. Chem. Phys.* 2009, **130**, 174713]. *J. Chem. Phys.* 2010, **133**, 049902.

58. Y. V. Suleimanov, R. Collepardo-Guevara and D. E. Manolopoulos, Bimolecular Reaction Rates from Ring Polymer Molecular Dynamics:Application to $H + CH_4 \rightarrow H_2 + CH_3$. *J. Chem. Phys.* 2011, **134**, 044131.

59. R. Pérez de Tudela, F. J. Aoiz, Y. V. Suleimanov and D. E. Manolopoulos, Chemical Reaction Rates from Ring Polymer Molecular Dynamics: Zero Point Energy Conservation in $Mu + H_2 \rightarrow MuH + H$. *J. Phys. Chem. Lett.* 2012, **3**, 493-497.

60. Y. V. Suleimanov, R. P. de Tudela, P. G. Jambrina, J. F. Castillo, V. Saez-Rabanos, D. E. Manolopoulos and F. J. Aoiz, A Ring Polymer Molecular Dynamics Study of the Isotopologues of the $H + H_2$ Reaction. *Phys. Chem. Chem. Phys.* 2013, **15**, 3655-3665.

61. J. W. Allen, W. H. Green, Y. Li, H. Guo and Y. V. Suleimanov, Communication: Full Dimensional Quantum Rate Coefficients and Kinetic Isotope Effects from Ring Polymer Molecular Dynamics for a Seven-Atom Reaction OH + CH_4 → CH_3 + H_2O. *J. Chem. Phys.* 2013, **138**, 221103.

62. Y. Li, Y. V. Suleimanov, J. Li, W. H. Green and H. Guo, Rate Coefficients and Kinetic Isotope Effects of the X + CH_4 → CH_3 + HX (X = H, D, Mu) Reactions from Ring Polymer Molecular Dynamics. *J. Chem. Phys.* 2013, **138**, 094307.

63. R. Pérez de Tudela, Y. V. Suleimanov, J. O. Richardson, V. Saéz Rábanos, W. H. Green and F. J. Aoiz, Stress Test for Quantum Dynamics Approximations: Deep Tunneling in the Muonium Exchange Reaction D + HMu → DMu + H. *J. Phys. Chem. Lett.* 2014, **5**, 4219-4224.

64. E. González-Lavado, J. C. Corchado, Y. V. Suleimanov, W. H. Green and J. Espinosa-Garcia, Theoretical Kinetics Study of the O(^{3}P) + CH_4/CD_4 Hydrogen Abstraction Reaction: The Role of Anharmonicity, Recrossing Effects, and Quantum Mechanical Tunneling. *J.Phys. Chem. A* 2014, **118**, 3243-3252.

65. J. Espinosa-García, A. Fernández-Ramos, Y. V. Suleimanov and J. C. Corchado, Theoretical Kinetics Study of the F(^{2}P) + NH_3 Hydrogen Abstraction Reaction. *J. Phys. Chem. A* 2014, **118**, 554-560.

66. Y. Li, Y. V. Suleimanov, W. H. Green and H. Guo, Quantum Rate Coefficients and Kinetic Isotope Effect for the Reaction Cl + CH_4 → HCl + CH_3 from Ring Polymer Molecular Dynamics. *J. Phys. Chem. A* 2014, **118**, 1989-1996.

67. Y. V. Suleimanov and J. Espinosa-García, Recrossing and Tunneling in the Kinetics Study of the OH + CH_4 → H_2O + CH_3 Reaction. *J. Phys. Chem. B* 2016, **120**, 1418-1428.

68. Y. V. Suleimanov, W. J. Kong, H. Guo and W. H. Green, Ring-Polymer Molecular Dynamics: Rate Coefficient Calculations for Energetically Symmetric (Near Thermoneutral) Insertion Reactions (X + H_2) → HX + H(X = C(^{1}D), S(^{1}D)). *J. Chem. Phys.* 2014, **141**, 244103.

69. K. M. Hickson, J.-C. Loison, H. Guo and Y. V. Suleimanov, Ring-Polymer Molecular Dynamics for the Prediction of Low-Temperature Rates: An Investigation of the $C(^1D) + H_2$ Reaction. *J. Phys. Chem. Lett.* 2015, **6**, 4194-4199.

70. K. M. Hickson and Y. V. Suleimanov, An Experimental and Theoretical Investigation of the $C(^1D) + D_2$ Reaction. *Phys. Chem. Chem. Phys.* 2017, **19**, 480-486.

71. J. Espinosa-García, C. Rangel and Y. V. Suleimanov, Kinetics Study of the $CN + CH_4$ Hydrogen Abstraction Reaction based on a New Ab Initio Analytical Full-Dimensional Potential Energy Surface. *Phys. Chem. Chem. Phys.* 2017, **19**, 19341-19351.

72. F. J. Aoiz, L. Bañares, J. F. Castillo, V. J. Herrero and B. Martínez-Haya, A Quasiclassical Trajectory and Quantum Mechanical Study of the $O(^1D)+D_2$ Reaction Dynamics. Comparison with High Resolution Molecular Beam Experiments. *Phys. Chem. Chem. Phys.* 2002, **4**, 4379-4385.

73. R. Grondin, J.-C. Loison and K. M. Hickson, Low Temperature Rate Constants for the Reactions of $O(^1D)$ with N_2, O_2 and Ar, *J. Phys. Chem. A,* 2016, **120**, 4838-4844.

74. N. Daugey, P. Caubet, B. Retail, M. Costes, A. Bergeat and G. Dorthe, Kinetic Measurements on Methylidyne Radical Reactions with Several Hydrocarbons at Low Temperatures. *Phys. Chem. Chem. Phys.* 2005**, 7**, 2921-2927.

75. N. Daugey, P. Caubet, A. Bergeat, M. Costes and K. M. Hickson, Reaction Kinetics to Low Temperatures. Dicarbon + Acetylene, Methylacetylene, Allene and Propene from $77 \leq T \leq 296$ K. *Phys. Chem. Chem. Phys.* 2008, **10**, 729-737.

76. R. J. Shannon, C. Cossou, J.-C. Loison, P. Caubet, N. Balucani, P. W. Seakins, V. Wakelam and K. M. Hickson, The Fast $C(^3P) + CH_3OH$ Reaction as an Efficient Loss Process for Gas-Phase Interstellar Methanol. *RSC Adv.* 2014, **4**, 26342-26353.

77. J. Bourgalais, M. Capron, R. K. A. Kailasanathan, D. L. Osborn, K. M. Hickson, J.-C. Loison, V. Wakelam, F. Goulay and S. D. Le Picard, The $C(^3P) + NH_3$ Reaction in Interstellar Chemistry. I. Investigation of the Product Formation Channels. *Astrophys. J.* 2015, **812**, 106.

78. K. M. Hickson, J.-C. Loison, J. Bourgalais, M. Capron, S. D. Le Picard, F. Goulay and V. Wakelam, The $C(^3P) + NH_3$ Reaction in Interstellar Chemistry. II. Low Temperature Rate Constants and Modeling of NH, NH_2, and NH_3 Abundances in Dense Interstellar Clouds. *Astrophys. J.* 2015, **812**, 107.

79. K. M. Hickson, J.-C. Loison, F. Lique and J. Kłos, An Experimental and Theoretical Investigation of the $C(^1D) + N_2 \rightarrow C(^3P) + N_2$ Quenching Reaction at Low Temperature. *J. Phys. Chem. A* 2016, **120**, 2504-2513.

80. K. M. Hickson, J.-C. Loison, D. Nuñez-Reyes and R. Méreau, Quantum Tunneling Enhancement of the $C + H_2O$ and $C + D_2O$ Reactions at Low Temperature. *J. Phys. Chem. Lett.* 2016, **7**, 3641-3646.

81. K. M. Hickson, J.-C. Loison and V. Wakelam, Temperature Dependent Product Yields for the Spin Forbidden Singlet Channel of the $C(^3P) + C_2H_2$ Reaction. *Chem. Phys. Lett.* 2016, **659**, 70-75.

82. D. Nuñez-Reyes and K. M. Hickson, Kinetic and Product Study of the Reactions of $C(^1D)$ with CH_4 and C_2H_6 at Low Temperature. *J. Phys. Chem. A* 2017, **121***,* 3851-3857.

83. Q. Y. Meng, K. M. Hickson, K. J. Shao, J.-C. Loison and D. H. Zhang, Theoretical and Experimental Investigations of Rate Coefficients of $O(^1D) + CH_4$ at Low Temperature. *Phys. Chem. Chem. Phys.* 2016, **18**, 29286-29292.

84. D. Nuñez-Reyes and K. M. Hickson, The Reactivity of $C(^1D)$ with Oxygen Bearing Molecules NO and O_2 at Low Temperature. *Chem. Phys. Lett.* 2017, **687***,* 330-335.

85. P. Bargueño, T. González-Lezana, P. Larrégaray, L. Bonnet, and J.-C. Rayez, Time Dependent Wave Packet and Statistical Calculations on the H+O_2 Reaction, *Phys. Chem. Chem. Phys.* 2007, **9**, 1127-1137.

86. P. Bargueño, T. González-Lezana, P. Larrégaray, L. Bonnet, J.-C. Rayez, M. Hankel, S. C. Smith and A. J. H. M. Meijer, Study of the H+O2 reaction by means of quantum mechanical and statistical approaches: The dynamics on two different potential energy surfaces, *J. Chem. Phys.* 2008, **128**, 244308.

87. A. J. Dobbyn and P. J. Knowles, A Comparative Study of Methods for Describing Non-adiabatic Coupling: Diabatic Representation of the $^1\sum^+/^1\Pi$ HOH and HHO Conical Intersections *Mol. Phys.* 1997, **91**, 1107-1124.

88. A. J. Dobbyn and P. J. Knowles, General Discussion. *Farad. Discuss.* 1998, **110**, 247.

89. P. Larrégaray, L. Bonnet and J.-C. Rayez, Validity of Phase Space Theory for Atom−Diatom Insertion Reactions. *J. Phys. Chem. A* 2006, **110**, 1552-1560.

90. P. Larrégaray, L. Bonnet and J.-C. Rayez, Mean Potential Phase Space Theory of Chemical Reactions. *J. Chem. Phys.* 2007, **127**, 084308.

91. Y. V. Suleimanov, J. W. Allen and W. H. Green, RPMDrate: Bimolecular Chemical Reaction Rates from Ring Polymer Molecular Dynamics. *Comput. Phys. Commun.* 2013, **184**, 833−840.

92. C. H. Bennett, In *Algorithms for Chemical Computations* Christofferson, R. E. Ed. ACS Symposium Series No. 46 American Chemical Society: Washington, DC, 1977 p 63.

93. D. Chandler, Statistical Mechanics of Isomerization Dynamics in Liquids and the Transition State Approximation. *J. Chem. Phys.* 1978, **68**, 2959-2970.

94. G. B. Pradhan, N. Balakrishnan and B. K. Kendrick, Quantum Dynamics of O(^{1}D)+D_2 Reaction: Isotope and Vibrational Excitation Effects. *J. Phys. B-At. Mol. Opt. Phys.* 2014, **47**, 135202.

95. M. Ahmed, D. S. Peterka and A. G. Suits, Crossed-beam Reaction of $O(^1D)+D_2 \rightarrow OD+D$ by Velocity Map Imaging *Chem. Phys. Lett.* 1999, **301**, 372-378.

96. J. Brandão and C. M. A. Río, Quasiclassical and Capture Studies on the $O(^1D)+H_2 \rightarrow OH+H$ Reaction using a New Potential Energy Surface for H_2O *Chem. Phys. Lett.* 2003, **377**, 523-529.

97. P. Casavecchia, Chemical Reaction Dynamics with Molecular Beams. *Rep. Prog. Phys.* 2000, **63**, 355-414.

98. J. A. Davidson, C. M. Sadowski, H. I. Schiff, G. E. Streit, C. J. Howard, D. A. Jennings and A. L. Schmeltekopf, Absolute Rate Constant Determinations for the Deactivation of $O(^1D)$ by Time Resolved Decay of $O(^1D) \rightarrow O(^3P)$ Emission. *J. Chem. Phys.* 1976, **64**, 57-62.

99. Z. P. Sun, S. Y. Lin and Y. J. Zheng, Adiabatic and Non-Adiabatic Quantum Dynamics Calculation of $O(^1D)+D_2 \rightarrow OD+D$ Reaction. *J. Chem. Phys.* 2011, **135**, 234301.

100. G. B. Pradhan, N. Balakrishnan and B. K. Kendrick, Ultracold Collisions of $O(^1D)$ and H_2: The Effects of H_2 Vibrational Excitation on the Production of Vibrationally and Rotationally Excited OH. *J. Chem. Phys.* 2013, **138**, 164310.